ORIGINAL ARTICLE

A developed system for melanoma diagnosis

Nadia Smaoui

Control and Energy Management laboratory
National School of Engineers of Sfax, Tunisia

Souhir Bessassi

Higher Institute of Computer Science and Multimedia of Gabes, Tunisia

Abstract

In recent years, there has been a fairly rapid increase in the number of melanoma skin cancer patients. Melanoma, this deadliest form of skin cancer, must be diagnosed early for effective treatment. So, it is necessary to develop a computer-aided diagnostic system to facilitate its early detection. In this paper, the proposed work is based on a combination of a segmentation method and an analytical method and aims to improve these two methods in order to develop an interface that can assist dermatologists in the diagnostic phase. As a first step, a sequence of preprocessing is implemented to remove noise and unwanted structures from the image. Then, an automatic segmentation approach locates the skin lesion. The next step is feature extraction followed by the ABCD rule to make the diagnosis through the calculation of the TDV score. In this research, three diagnosis are used which are melanoma, suspicious, and benign skin lesion. The experiment uses 40 images containing suspicious melanoma skin cancer. Based on the experiment, the accuracy of the system is 92% which reflects its viability.

Keywords: melanoma, segmentation, skin cancer, ABCD rule

1. INTRODUCTION

Skin cancer is considered as the most common form of cancer worldwide. The incidence is considerably increasing. For example in the US, at current rates, a skin cancer will develop in one in five people during their lifetime [1]. Skin cancers can be classified into two major groups which are melanoma and non-melanoma skin cancers. These type of skin cancer (non-melanoma) is usually start in the basal cells or squamous cells. Such cells are found at the base of the outer layer of the skin. Approximately 1,200,000 non-melanoma skin cancers develop in the US. The Exposure of the skin to sunlight is considered as the main factor behind the development of the most basal and squamous cell cancers. Basal cell or squamous cell cancers can be cured if found and treated early. Melanoma is the most dangerous type of skin cancer [1]. The World Health Organization approximates that more than 70230 people a year in the world die from too much sun, mostly from malignant skin cancer [2]. Early detection of this cancer can help its curability. Melanoma arises from the cancerous growth in the pigmented spots. Dermatologists can diagnose melanoma

in about 80% of cases according to ABCD process [3]. Digital dermatoscopy could give dermatologists a closer look at suspicious skin lesions. This, in turn, can help dermatologists to find suspicious lesions in an early step. To measure and detect sets of features from dermoscopic images, the computerized analysis of these images can be extremely useful and helpful for dermatologists in order to facilitate their diagnosis. Based on images obtained by digital dermoscopy, our conclusive aim is to develop an aided-diagnostic system for the identification of early stage melanomas. This would enable supervised classification of melanocytic lesions. The melanoma detection process is composed of five steps that are the preprocessing, the segmentation, the post-processing, the feature extraction by the ABCD rule and finally the classification based on the Total Dermatoscopic Value calculation (TDV). The ABCD rule presents the following features which are the Asymmetry, the Border Irregularity, the Color variation and the Diameter. This latter must be greater than 6mm in the case of melanoma. This paper is organized as follows. In Section 2 we present a brief overview of previous related work. In Section 3, we illustrate our approach to melanoma skin cancer detection. Experimental results and analysis are presented and discussed in Section 4. Finally, we present

---

*Corresponding author

a brief conclusion.

2. Melanoma skin cancer detection: State of the Art

Melanoma is considered as the most rapidly proliferating cancers in the world [4]. For that, there has been a significant increase in concern in the development of automatic digital dermatoscopic image analysis methods. Among these methods, the color enhancement which is based on the color correction with HSV model. In this approach, linear regression models are constructed for each channel, which allows automatic adjustment of the hue and saturation [5]. A second approach is based on a scheme of standardization based on two steps; removing the color variations and strengthening contrast images [6]. Although this approach has in some cases good results, it remains limited since lesions classification depends on other parameters like asymmetry and border irregularity.

Other approaches developed in the literatures are based on feature extraction. The first describes a new method based on graphs which will enable networks to extract pigments from images of dermoscopy [7].The second implements the classification of skin lesions based on the characteristics of "granularity" [8]. The third proposes a classification with white areas on the images [9]. The last method extracts the characteristics of curvature from 3D images acquired using a photometric stereo system [9].

Another method is widely adopted by researchers. This method consists, generally, of four stages which are: acquisition, segmentation , feature extraction and classification.The segmentation is the most difficult step since it affects the precision of the subsequent stages and because [4]: (i) The transition between the lesion and the healthy skin is usually of low contrast; (ii) the borders of the lesion are usually fuzzy and irregular; (iii) the presence of complicating artifacts. To resolve these problems, several segmentation algorithms have been developed. We can classify these into three categories which are edge contour-based, thresholding and region-based.

An effective thresholding method proposed by Grana et al. [10] is based on Otstu thresolding algorithm. It aims at segmenting automatically the melanoma image. Then, the developed method selects k points for spline-based interpolation,which gives a smooth edge of lesion. Such methods achieve good results when there is good contrast between lesion and skin, but face problems when there is an overlap of the modes of the two regions.

Edge/ contour-based approaches were used in [11][12]. Rubegni et al. [11] segmented dermoscopy images using the zero-crossings of a LoG edge operator, while Zhou et al. [12] used an improved snake model to detect lesion borders. Edge and contour-based approaches perform poorly when the boundaries are not well dened, for instance when the transition between skin and lesion is smooth. In such
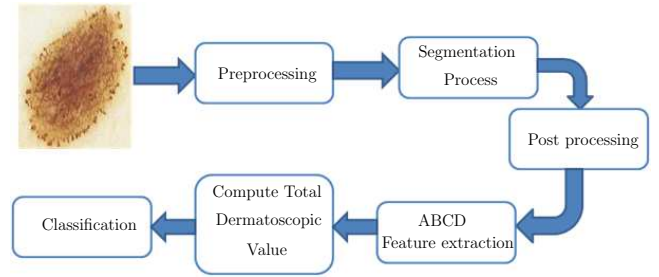

Figure 1: Architecture System of Melanoma Skin Cancer Diagnosis

situations, the edges have gaps and the contour may leak through them.

Region-based approaches have also been used. Some examples include multi-scale region growing [13], fuzzy c-means based on anisotropic mean shift [14], multi- resolution markov random elds [15]. The researchers presented by Fatichah et al. [16][17] segmented the skin lesion using fuzzy region growing and the diagnoses are based on ABCD feature which is used to diagnose melanoma skin cancer based on Total Dermatoscopic Value (TDV).Based on the experiment using 30 samples images, the accuracy of the system proposed by Fatichah et al. [16] is 85% but the accuracy using fuzzy region growing proposed by Fatichah et al. [17] is 86.6%.

Despite region-based approaches have difculties, especially, when the lesion or the skin region are textured, this category is widely used by researchers. For that, in this paper we try to improve region growing algorithm for the detection of lesion.

3. Architecture System of Melanoma Skin Cancer Detection

The processing algorithm presented in Fig. 1 describes the melanoma skin cancer detection. Dermatoscopic images used in this work are collected with the Department of Dermatology, University Hospital Hedi Chaker Sfax. They are coded on 24 bits storing the three color components r (red), g (green) and b (blue). These rgb images are 640x480 pixels in size. Unfortunately, the image acquisition leads to the permanent presence of illumination. The existence of shadows, reflections on wet tissue or fatty report more difficulties. In addition, artifacts such as hair and diversity of skin color complicate the acquisition step and make it difficult to reproduce. These constraints illumination and noise justify the importance of the preprocessing algorithm used thereafter.

3.1. Preprocessing

As mentioned, the image preprocessing is an important step in image diagnosis. It is used to correct defects illumination, eliminating noise and small spots and enhance
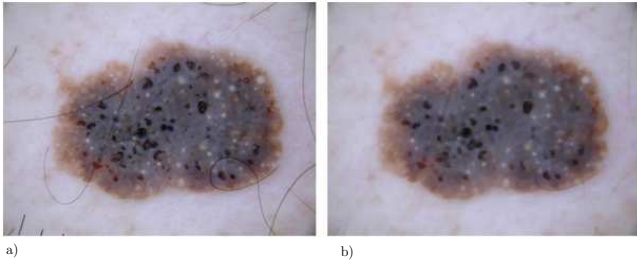
Figure 2: Preprocessing: (a) Original image (b) image given after applying the median filter and the morphological closing
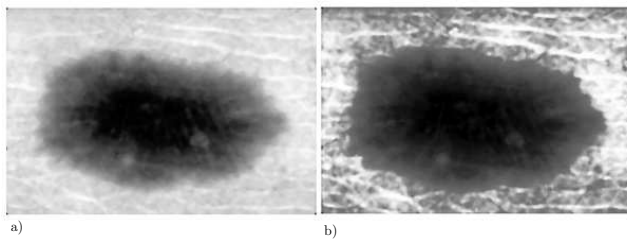

Figure 3: Influence of the histogram adjustment on grayscale image:(a) Filtered image converted to grayscale (b) Influence of the histogram adjustment

Figure 4: Automatic method for the choice of the germ

the contours and contrast as much as possible without degrading the lesion. Preprocessing proposed in this work is composed of three steps. It starts by using a median filter aiming at cleaning the image by eliminating certain defects. This spatial filter is based on calculating for each pixel the median of the gray levels of the neighbors pixels. Since each component of the image can be viewed as a grayscale image, we can apply this filter on each component separately. Then, we performed a morphological closing aiming at eliminating all artifacts such as hair. According to the images provided, it was found empirically that setting a 5x5 median filter and a disk with a diameter of 3 gives the best results. Fig. 2 shows the influence of the median filter and the morphological closing on the image.

Finally, we must improve the color between the lesion and healthy skin. Since our goal is to extract the lesion apart, we improve the contrast of the image by adjusting intensity values after converting the image to grayscale. The influence of the Histogram adjustment on the grayscale image is shown in Fig. 3.

3.2. Segmentation

To do a classification of skin lesions, and particularly to distinguish melanoma from benign lesions, we must begin by isolating the lesion from healthy skin that surrounds each color image using a segmentation methodology. The detection of this skin lesion is a critical problem in dermatoscopic images because the transition between the lesion and the surrounding skin is difficult to detect accurately. For this, segmentation method chosen must be pre-
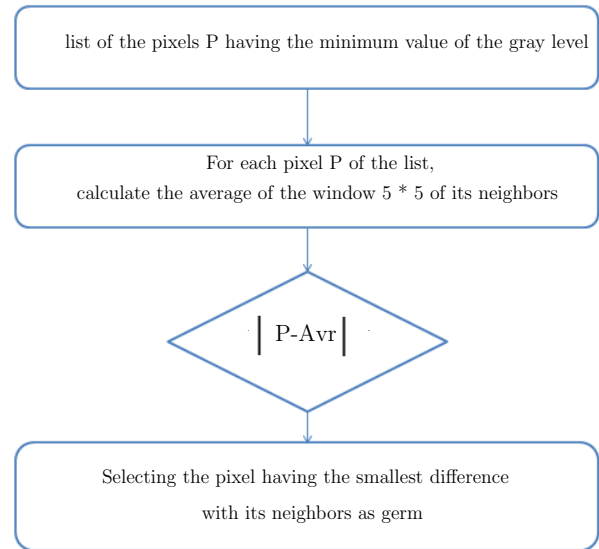
cise. In this paper, the segmentation process used is region growing. This segmentation technique begins with a pixel as the seed point. Then it aggregates the pixels according to two criteria: homogeneity and adjacency [18]. Several studies have used the segmentation by region growing to detect skin lesions. Fondn et al. [19] have described a method based on selecting a region with the mouse. The selection of this region can then make the choice of the seed point and the stop criterion. Fatichah et al. [16] described a method using the center of a homogenous area as the germ and fixing the threshold randomly. These two manual methods, based on a random selection of the threshold and the germ, are not recommended. In fact, it will have a bad Influence on the segmentation result.

In this work, we tried to adapt a simple method of region growing for our application to detect skin lesions. To optimize the result of the segmentation, the proposed method is based on an automatic choice of the threshold and the seed point from which and at each level of growth we add the neighboring pixels having similar properties.

Since only one region must be segmented and the lesion is always darker than the normal skin, the seed pixel will be automatically selected as the pixel with the gray level which is darker and more similar to its neighbors. This characteristic is achieved by calculating the difference between the pixel P and the average of a 5x5 window of its neighbors. This method is illustrated in the diagram presented in Fig. 4.

The result is shown in Fig. 5 where in Fig. 5(a) pixels having the darkest gray level are selected. Then, the seed pixel is detected in Fig. 5(b).

After selecting the seed pixel, the application of this algorithm includes a specification of two variables that are the size of the window and the threshold. The size of the
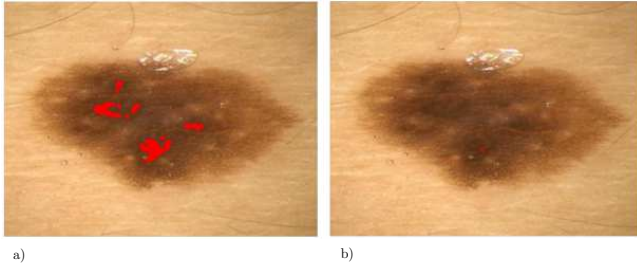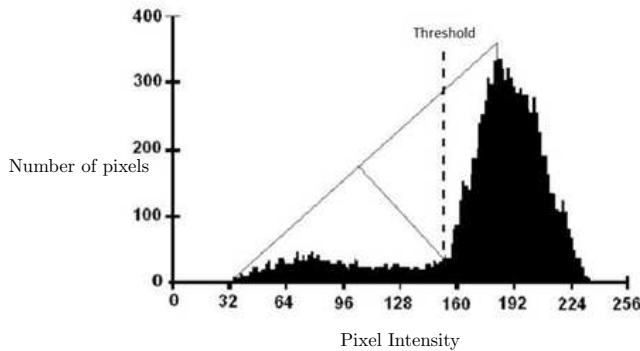
Figure 5: The seed pixel selection

Figure 6: Triangle method

window is set to 3x3 pixels since it gives best result. The threshold is calculated using the following steps:

*Finding the optimal threshold S of the image automatically using the triangle method [20] which allows constructing a line between the histogram peak and the farthest end. The threshold is the maximum distance between the line and the histogram as shown in Fig. 6. The choice of this method is based on the fact that all the images showing a lesion are still presented as a dark spot surrounded by a lighter area (skin) as shown in Fig. 7(a). The histogram of such an image is always given as presented in Fig. 7(b)
.

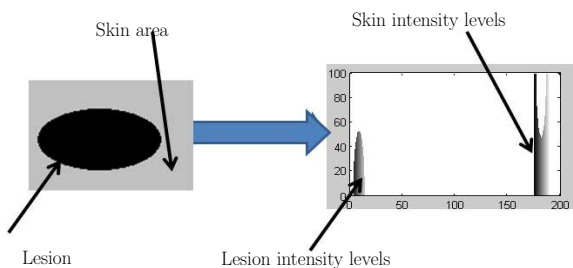*Calculating the average of the region where N is the

Figure 7: Choice of the triangle method:a) An image presenting a lesion,b) Corresponding histogram

number of pixels belonging to the region:

$$Avr = \frac{\sum values \ of \ the \ pixels \ belonging \ to \ the \ regions}{N} \quad (1)$$

*The threshold is calculated by measuring the difference between the average and the optimal threshold

$$Threshold = |Avr - S| \quad (2)$$

Then, the growth process used the following steps:
*Step 1: Adding the seed point neighboring pixels belonging to a window of 3x3 pixels to a list of neighbors.
*Step 2: Calculating the difference between the graylevel of each neighboring pixel and the region average.
*Step 3: Adding the neighboring pixel of the seed point, with the smallest difference, in the region and mark it as a seed pixel.
*Step 4: Updating the average Avr, the threshold and the gray level difference.
*Step 5: Deleting the pixel from the list of neighbors
*Step 6: Returning to step 1 each time the difference found in step 4 is less than the threshold.
Hence, the approach is to grow the region around the starting pixel. This aggregation does not stop until the difference exceeds a certain threshold:

$$|I(x,y) - Avr| >= threshold \quad (3)$$

3.3. Post processing

To remove isolated pixels within the region of the lesion by the segmentation, a further step of morphological closing is produced. In our work, the disc diameter of this morphological closing is set to 5 as it gives the best result. Finally, the resulting image is a binary mask used to separate the lesion from the skin. It is then superimposed with the original image. Fig. 8 illustrates this step.

3.4. ABCD feature extraction

The ABCD rule was introduced by Stolz et al. [21] and used by dermatologists in recognition process of skin lesions to assess the risk of malignity of a pigmented lesion. This method is able to provide a more objective and reproducible diagnostic of skin cancers in addition to its speed of calculation.It is based on four parameters: A (Asymmetry) concerns the result of evaluation of lesions asymmetry, B (Border) estimates the character of lesions border, C (Color) identifies the number of colors present in the investigated lesion, and D (Diameter).

3.4.1. Asymmetry

The asymmetry of the lesion is the most important indicator characterizing the malignancy. This characteristic is considered in terms of form and color. To facilitate the task of calculating the score of asymmetry, we translated the lesion to the center of the image. Then we rotate the lesion to align the major axis horizontally as presented in Fig. 9.
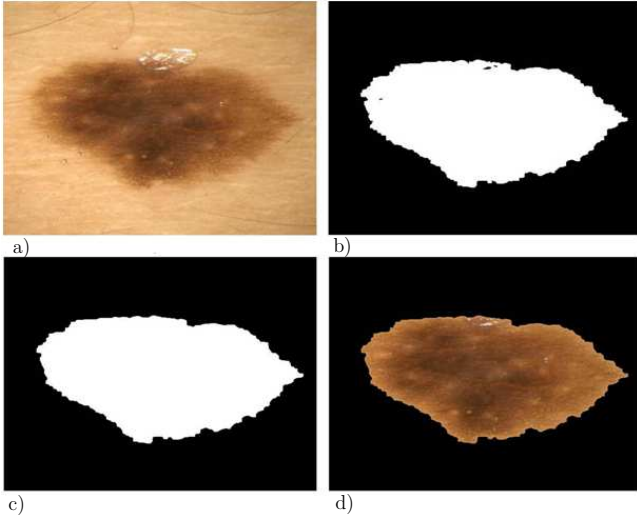
Figure 8: The result of the segmentation: (a) original image (b) lesion detected by region growing (c) lesion detected after post-processing (d) segmented image
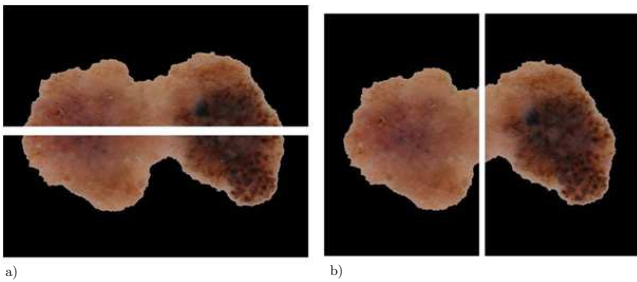

Figure 9: The division of the lesion: (a) according to the major axis (b) According to the minor axis

Now it is easy to divide the image according to the major axis and the minor axis of the lesion (Fig. 9). To measure the asymmetry in terms of form, we are basing our calculation on the asymmetry index presented as follows [22].

$$AI = \sum_{k=1}^{2} \frac{\Delta Ak}{AL} \qquad (4)$$

where k is the major axis and the minor axis ΔAk is the area of non-overlapping zone and AL is the total area of the lesion.

To measure the asymmetry in terms of color, our calculations are based on the histograms of the three RGB components of each part of the lesion and the chi-square distance.

$$D(h1, h2) = \sum_{i=1}^{N} \frac{(h1(i) - h2(i))^2}{h1(i) + h2(i)} \qquad (5)$$

where $h1$ and $h2$ are the two histograms of size N.

Figure 10: Calculating the border score: B=3

Finally, the asymmetry score A is calculated as the average between the asymmetry score in terms of form and that in terms of color.

3.4.2. Border Irregularity

Generally, the borders of the benign lesions are clearly defined. The irregularity of the border can usually report a cancer during growth and propagation. For an evaluation, the lesions are divided into eight sectors as presented in Fig. 10. Within each sector, a strong and sharp cut pattern at the periphery receives a score of 1. In contrast, a gradual approach, indistinct within each segment has a score of 0. Thus, the maximum irregular border score is 8, and the minimum one is 0. This calculation is based on the Euclidean distance and the standard derivation in each sector.

$$Di = \sqrt{(x2 - x1)^2 + (y2 - y1)^2} \qquad (6)$$

where $x2$ and $y2$ are the coordinates of the center of the lesion. $x1$ and $y1$ are the coordinates of pixel i.

$$Distance = \sum_{i=1}^{N} Di \qquad (7)$$

With N is the number of pixels in the edge belonging to the considered area. Di is the Euclidean distance between the center of the lesion and the pixel i.

Then the standard deviation is calculated for each sector with the following equation:

$$s = (\frac{1}{N} \sum_{i=1}^{N} (xi - x)2)^{1/2} \qquad (8)$$

where n is the number of elements in the sector.

Within each sector, if the deviation exceeds a certain threshold, the score edge is 1. This threshold is set empirically to 30.

3.4.3. Colors

Melanomas are characterized by the presence of six different colors, namely, white, red, light brown, dark brown, blue-gray and black. For each present color, we add 1 to the score. When the six colors are present, the maximum score is 6. The minimum score is 1.To verify the existence

Figure 11: Color score calculation for a lesion:C=2(light brown and dark brown)

Figure 12: The scales used to measure the actual diameter

of each color in the lesion,the image was converted from the RGB color space to the CIE Labcolor space because the distance between two colors in the RGB color space does not reflect the "difference" perceived by the naked eye contrary to the CIE Labcolor space. This difference can be calculated using the Euclidean distance delta E.

$$\Delta E = \sqrt{(L1 - L2)^2 + (a1 - a2)^2 + (b1 - b2)^2} \quad (9)$$

where $L1$, $a1$ and $b1$ are the components of the CIE Lab colorimetric space of the desired color and $L2$, $a2$ and $b2$ those of each pixel of the image.
The smallest perceptible difference is known 'Just Noticeable Difference' (JND) [23]. It is fixed to 2.3. In practice, to consider two colors are equivalent, tolerance can be set at 3 * JND. The Fig. 11 shows the result for a lesion.

3.4.4. Diameter

Since the dermatoscope gives the possibility of tracing the marks on the image during acquisition (Fig. 12), we are based on these scales to calculate the actual diameter of the lesion.

We note that the lesion diameter greater than 6 millimeters is more likely to be malignant than a small lesion.

3.5. Classification

After obtaining the values of the four characteristics, the Total Dermatoscopic value (TDV) is calculated based on the following formula where each one of the presented characteristics is multiplied by a weighting factor:

$$TDS = 1.3 * A + 0.1 * B + 0.5 * C + 0.5 * D \quad (10)$$

This score contributes to detect benign or malignant pigmented skin lesion as presented as follows:
    $*TDS < 4.75$: Benign skin lesion

$*4.75 \leq TDS \leq 5.45$: Suspicious
In this case, the intervention of the doctor is required by removing the suspicious lesion (biopsy) followed by its microscopic examination (histology). In general, dermatologists prefer to immediately remove the entire lesion, but in some cases, a partial biopsy may be performed.
    $*TDS > 5.45$: Melanoma

4.   Experimental results and analysis

In the experiment, the dermatoscopic image suspected as melanoma is used as input data. To evaluate the performance of our developed system, this research use dataset of 40 dermatocospic images. The measures used for the evaluation are accuracy, sensibility and specificity measures presented as follows,

$$Accuracy = \frac{(Number\ of\ detected\ lesions)}{(Number\ of\ images\ in\ the\ dataset)} * 100 \quad (11)$$

$$Sensivity = \frac{TP}{TP + FN} \quad (12)$$

$$Specificity = \frac{TN}{TN + FP} \quad (13)$$

where TP is the number of true positives, FN the number of false negatives, TN the number of true negative, and FP the number of false positives. A positive result is a lesion which is classified as malignant and a negative result is a lesion that is classified as benign. The sensitivity and specificity measure the percentage quoted classifications specific for malignant and benign cases, respectively. our work is based on 40 images (27 malignant and 13 benign lesions). The experimental results of total dermatocospic images is described in the following Table.

Table 1: Accuracy result

Measure	Accuracy	Sensitivity	specificity
Experimental Result	92.5%	88.88%	92.3%

To facilitate the use of our application, we have implemented a graphical user interface presented in Fig. 13:

Figure 13 shows the main interface of our application which allows the user to select an image using the 'open'
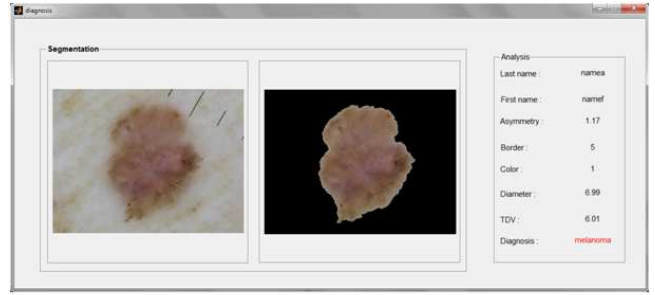
Figure 13: The Main user interface of the system

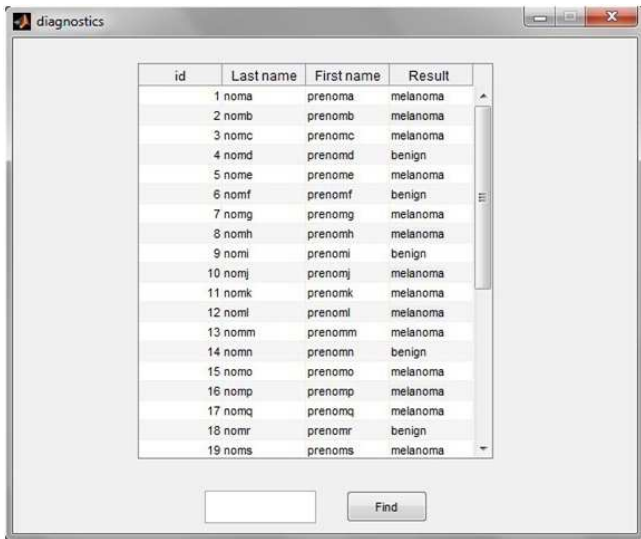
Figure 15: The TDV result user of the interface

Figure 14: The interface containing the list of patients in the database

Figure 16: Graphical interface results

command in the 'File' menu. Then he can use the 'Segment' command to detect the lesion from the healthy skin and display the results for the analysis and diagnosis. The user can either use the 'Save' command from the 'Diagnostics' menu to save the image in the database, or the 'View' command to view the results already achieved. The 'View' command opens the interface shown in Fig. 14.

The 'Search' button allows the user to search the record with the ID typed in the text box to display all the details such as image, name of the patient, the characteristics of the lesion (Asymmetry, Border, colors, Diameter and TDS) and the diagnostic in the interface of Fig. 15.

To evaluate our developed interface, we have tested the 40 images collected with the Department of Dermatology of the University Hospital Hedi Chaker Sfax, Tunisia.

Fig. 16 shows the results found by our interface compared against the diagnosis of dermatologist for two images.

As was mentioned, the accuracy of the system is about 92%. Based on the experimental results, the small value

of color variation causes, in some cases false diagnosis. To improve this accuracy, we must tuning the calculation of this parameter. We can use for example a color clustering model for dermoscopic images.

5. Conclusions

The objective of our work has involved the detection of melanoma based on region growing segmentation and the ABCD rule used for the detection of malignancy of pigmented skin lesion. The use of region growing in our method based on automatic selection of the seed pixel and the threshold ensures the best results and avoids overlap between the lesion and healthy skin. The result of the segmentation was then used in the next step by the ABCD rule in order to classify pigmented skin lesion as benign or malignant. There are three diagnosis that are used in this research i.e. melanoma, suspicious, and benign skin lesion. The experiment uses 40 samples of dermatoscopic images containing a lesion that is suspicious melanoma skin cancer. Based on the experiment, the accuracy of the system is 92% with 4 false diagnosis of the 40 samples. For illustration, we have developed a graphical interface in order to facilitate the diagnostic task for the dermatologists.

References

[1] S. Stechschulte, C. Ricotti, C. J. Cockerell, Advances in diagnostic testing for skin cancer, TOUCH BRIEFINGS (2008) 73–76.

[2] R.Lucas, T.McMichael, W.Smith, B.Armstrong, Solar ultraviolet radiation.global burden of disease from solar ultraviolet radiation, Environmental Burden of Disease. Series 13 (2006) 117.

[3] D.Rigel, J.Russak, R.Friedman, The evolution of melanoma diagnosis, A Cancer Journal for Clinicians 60 (2010) 301316.

[4] F. Xie, A. Bovik, Automatic segmentation of dermoscopy images using self-generating neural networks seeded by genetic algorithm, Pattern Recognition, ELSEVIER (2013) 1012–1013.

[5] H. Iyatomi, M. E. Celebi, G. Schaefer, M. Tanaka, Automated color calibration method for dermoscopy images, Computerized Medical Imaging and Graphics (2011) 89–98.

[6] G. Schaefer, M. I. Rajab, M. E. Celebi, H. shi Iyatomi, Colour and contrast enhancement for improved skin lesion segmentation, Computerized Medical Imaging and Graphics (2011) 99–104.

[7] M. Sadeghi, M. Razmara, T. K. Lee, M. Atkins, A novel method for detection of pigment network in dermoscopic images using graphs, Computerized Medical Imaging and Graphics (2011) 137–143.

[8] W. V. Stoecker, M. Wronkiewiecz, R. Chowdhury, R. J. Stanley, J. Xu, A. Bangert, B. Shrestha, D. A. Calcara, H. S. Rabinovitz, M. Oliviero, F. Ahmed, L. A. Perry, R. Drugge., Detection of granularity in dermoscopy images of malignant melanoma using color and texture features, Computerized Medical Imaging and Graphics (2011) 144–147.

[9] A. Dalal, R. H. Moss, R. J. Stanley, W. V. Stoecker, K. Gupta, D. A. Calcara, J. Xu, B. Shrestha, R. Drugge, J. M. Malters, L. A. Perry, Concentric decile segmentation of white and hypopig- mented areas in dermoscopy images of skin lesions allows discrimination of malignant melanoma, Computerized Medical Imaging and Graphics (2011) 148–154.

[10] C. Grana, G. Pellacani, R. Cucchiara, S. Seidenari, A new algorithm for border description of polarized light surface microscopic images of pigmented skin lesions, IEEE Transactions on Medical Imaging 22 (2003) 959964.

[11] P. Rubegni, A. Ferrari, G. Cevenini, D. Piccolo, M. Burron, Differentiation between pigmented spitz naevus and melanoma by digital dermoscopy and stepwise logistic discriminant analysis, Melanoma Research 11 (2001) 3744.

[12] H. Zhou, G. Schaefer, M. C. nad F. Lin, T. Liu, Gradient vector ?ow with mean shift for skin lesion segmentation, Computerized Medical Imaging and Graphics 35 (2011) 121127.

[13] W. S. M.E. Celebi, A. Aslandogan, Unsupervised border detection in dermoscopy images, Skin Research and Technology 13 (2007) 454462.

[14] H. Zhou, G. Schaefer, A. Sadka, M. Celebi, Anisotropic mean shift based fuzzy c-means segmentation of dermoscopy images, IEEE Journal of Selected Topics in Signal Processing 3 (2009) 2634.

[15] J. Gao, J. Zhang, M. Fleming, A novel multiresolution color image segmen- tation technique and its application to dermatoscopic image segmentation, Proceedings of the IEEE International Conference on Image Processing Vancouver, BC, Canada (2000) 2634.

[16] B.Amalian, C.Fatichah, M.R.Widyanto, Abcd feature extraction for melanoma skin cancer diagnosis, Proceedings of the 9th International Conference on Advanced Computer Science and Information System (2009) 224228.

[17] M.R.Widyanto, C.Fatichah, B.Amaliah, Skin lesion detection using fuzzy region growing and abcd feature extraction for melanoma skin cancer diagnosis, http://www.its.ac.id/personal/files/pub/ (2013) 4554–chastine–Full.

[18] H.Laguel, Deploiement sur une plateforme de visualisation, d'un algorithme cooperatif pour la segmentation d'images irm base sur les systemes multiagents, University of Science and Technology Houari Boumediene,Algeria (2010) 1–104.

[19] I.Fondn, C.Serrano, B.Acha, Segmentation of skin cancer images based on multistep region growing, MVA2007 IAPR Conference on Machine Vision Applications (2007) 339–342.

[20] S.Latt, G.Zack, W.Rogers, Automatic measurement of sister chromatid exchange frequency, Thejournal of histochemistry and cytochemistry Volume 25 (1977) 741–753.

[21] W.Stolz, Abcd rule of dermatoscopy: a newpractical method for early recognition of malignant melanoma, European Journal of Dermatology, Volume 4 (1994) 521–527.

[22] M.R., Widyanto, C. Fatichah, B. Amaliah, Abcd feature extraction for melanoma skin cancer diagnosis, Proceedings of the 9th International Conference on Advanced Computer Science and Information System (2009) 224–228.

[23] O.Kakde, K.Bhoyar, Color image segmentation based on jnd color histogram, International Journal of Image Processing (IJIP), Volume 3 (2010) 283–292.